Chapter 3
Methodologies for UHI Analysis

Urban Heat Island Phenomenon and Related Mitigation Measures in Central Europe

Ardeshir Mahdavi, Kristina Kiesel, and Milena Vuckovic

Abstract A central strand of research work in the realm of urban physics aims at a better understanding of the variance in microclimatic conditions due to factors such as building agglomeration density, anthropogenic heat production, traffic intensity, presence and extent of green areas and bodies of water. The characteristics and evolution of the urban microclimate is not only relevant to people's experience of outdoor thermal conditions in the cities. Higher air temperatures also exacerbate discomfort caused by the overheating of indoor spaces and increases cooling energy expenditures. It can be argued that the solid understanding of the temporal and spatial variance of urban microclimate represents a prerequisite for the reliable assessment of the thermal performance of buildings (energy requirements, indoor thermal conditions). In this context, the present treatment entails a three-fold contribution. First, the existence and extent of the UHI phenomena are documented for a number of Central-European cities. Second, a comprehensive assessment of the effectiveness of UHI mitigation measures in these cities is described that is conducted using advanced numeric modelling instruments. Third, a systematic framework is proposed to identify a number of variables of the urban environment that are hypothesized to influence UHI and the urban microclimate variance. These variables pertain to both geometric (morphological) and semantic (material-related) urban features.

Keywords Urban climate • Urban heat island • Mitigation measures • Simulation • Evaluation

A. Mahdavi (✉) • K. Kiesel • M. Vuckovic
Department of Building Physics and Building Ecology, Vienna University of Technology, Vienna, Austria
e-mail: bpi@tuwien.ac.at

F. Musco (ed.), *Counteracting Urban Heat Island Effects in a Global Climate Change Scenario*, DOI 10.1007/978-3-319-10425-6_3

3.1 Introduction

The characteristics of the urban microclimate are of critical importance with regard to inhabitants' health and well-being (thermal comfort, heat stress, mortality rates) as well as energy and environmental issues (Akbari 2005; Harlan and Ruddell 2011). In the last few years, the general awareness concerning the urban microclimate has been steadily rising. However, given the fact that world-wide an increasing number of people live in cities, further research and planning efforts are needed to better understand and address the effects of urban microclimate, its variance, and its development. Given the complexity of the urban fabric, it is widely recognized that heat storage in urban areas will be higher when compared to unbuilt areas (Grimmond and Oke 1999; Piringer et al. 2002). Generally speaking, the undesired thermal circumstances in the urban environment are caused in part by certain properties of the materials used for construction of buildings, pavements, and roads, the urban layout and structure including topography, morphology, density, and open space configuration, as well as processes and activities such as transportation and industry (Unger 2004; Grimmond 2007; Alexandri 2007; Kleerekoper et al. 2012; Shishegar 2013). These factors can affect, amongst other things, the way solar radiation is absorbed by urban surfaces and the way air masses flow through the urban fabric. Empirical observations in many cities around the world point to significantly higher urban temperatures than the surrounding rural environment. This circumstance is referred to as the urban heat island (UHI) phenomenon (see, for example, Voogt 2002; Arnfeld 2003; Blazejczyk et al. 2006; Oke 1981; Gaffin et al. 2008). Together with climate change, this phenomenon can be crucial to the way we view urban areas as living environments.

Recently, a number of research efforts have been initiated to better understand the very specifics of the UHI phenomenon (see, for example, Arnfeld 2003; Blazejczyk et al. 2006). Some of related foci of these efforts are to describe the characteristics and patterns of UHI (Voogt 2002; Hart and Sailor 2007). Empirical observations have shown that the UHI phenomenon shows different characteristics during different seasons (Gaffin et al. 2008) and that it is pronounced differently during the night and the day (Oke 1981). Furthermore, the intensity of urban heat islands is believed to rise proportionally to the size and population of the urban area (Oke 1972). More recently, Gaffin et al. (2008) performed a detailed spatial study of New York City's current UHI and concluded that summer and fall periods were generally the strongest UHI seasons, consistent with seasonal wind speed changes in the area. A simple quantitative indicator of urban heat island phenomenon is the UHI intensity. The UHI intensity is defined as the difference between urban and rural air temperature (Oke 1972).

Generally, heat island intensities are quantified in the range of 1–3 K, but under certain atmospheric and surface conditions can be as high as 12 K (Voogt 2002). Material properties of urban surfaces (Grimmond et al. 1991; Akbari et al. 2001) as well as evapotranspiration, and anthropogenic heat emission (Taha 1997) can result in higher urban temperatures. To address the implications of the UHI phenomenon, cities (both governmental bodies and affected stakeholders) must implement well-conceived, comprehensive, and collective actions with a high potential to positively influence urban climate and remedy the negative phenomena associated with the urban heat islands.

In this context, the present contribution reports on the results of data analyses and modelling efforts undertaken to investigates the extent of urban heat island phenomena and the potential of relevant mitigation measures in the Central European region (Mahdavi et al. 2013). Thereby, a large set of data was collected and analysed concerning the extent of the UHI effect in multiple cities in Central Europe. Furthermore, to develop and demonstrate approaches toward supporting the process of design and evaluation of UHI mitigation measures, the potential of numerical (simulation-based) urban microclimate analysis models were explored.

As numerical modelling poses certain challenges not only in view of time and computational resources but also model validation and calibration issues, the potential of alternative (or complementary) empirically-based modelling options were investigated. To develop such alternative models, certain features of the urban environment are hypothesized to influence UHI and the urban microclimate variance. The related variables, which pertain to both geometric (morphological) and semantic (material-related) urban features are captured within a systematic framework.

The statistical relationships between the values of such variables and the extent of microclimatic variance provide the basis for simple empirically-based models. These models can be directly used to predict the impact of mitigation measures or indirectly applied to gauge the performance of detailed numerical models of the urban microclimate.

3.2 The Urban Heat Island in Central Europe

Metropolitan areas worldwide vary in their spatial configuration. This is typically manifested in the diversity of the respective microclimatic conditions. The present contribution focuses on documenting this diversity in terms of the frequency, magnitude, and time-dependent (diurnal and nocturnal) UHI intensity distribution (during a reference week) and the long-term development of urban and rural temperatures in seven Central-European cities, namely Budapest, Ljubljana, Modena, Padua, Prague, Stuttgart, Vienna, and Warsaw (see Tables 3.1 and 3.2). The magnitude of the UHI effect can be expressed in terms of Urban Heat Island intensity (UHI). This term denotes the temperature difference (in K) between simultaneously measured urban and rural temperatures. The aim was to identify and evaluate the extent of the UHI effect and its variance in the broader geographical context of the participating cities.

As already mentioned, UHI intensity in observed urban areas was derived for a reference summer week (with high air temperature and relatively low wind velocity) selected by each participating city independently. The collected information included hourly data on air temperature, wind speed, and precipitation from two representative weather stations (one urban and one rural).

Table 3.1 General information about the participating cities

City	Area [km^2]	Population [millions]	Latitude	Longitude	Altitude [m]
Budapest	525	1.74	47° 30' N	19° 3' E	90–529
Ljubljana	275	0.28	46° 3' N	14° 30' E	261–794
Modena	183	0.18	44° 39' N	10° 55' E	34
Padua	93	0.21	45° 25' N	11° 52' E	8–21
Prague	496	1.26	50° 5' N	14° 25' E	177–399
Stuttgart	207	0.60	48° 46' N	9° 10' E	207–548
Vienna	415	1.73	48° 12' N	16° 22' E	151–543
Warsaw	517	1.70	52° 13' N	21° 00' E	76–122

Table 3.2 Information about the urban topology of the participating cities

City	Topology
Vienna	Vienna is located in north-eastern Austria, at the eastern most extension of the Alps in the Vienna Basin.
Stuttgart	Stuttgart's center lies in a Keuper sink and is surrounded by hills. Stuttgart is spread across several hills, valleys, and parks.
Padua	Padua is located at Bacchiglione River, 40 km west of Venice and 29 km southeast of Vicenza. The Brenta River, which once ran through the city, still touches the northern districts. To the city's south west lie the Euganaean Hills.
Budapest	The Danube River divides Budapest into two parts. On the left bank the Buda is located, with over 20 hills within the territory of the capital, and on the right bank the flat area of Pest is located with its massive housing, as well as commercial and industrial areas.
Prague	Prague is situated on the Vltava river in the center of the Bohemian Basin.
Modena	Modena is bounded by the two rivers Secchia and Panaro, both affluent of the Po River. The Apennines ranges begin some 10 km from the city, to the south.
Warsaw	Warsaw is located some 260 km from the Baltic Sea and 300 km from the Carpathian Mountains. Furthermore, Warsaw is located in the heartland of the Masovian Plain.
Ljubljana	Ljubljana is located in the Ljubljana Basin between the Alps and the Karst Plateau.

To obtain a long-term impression of the urban and rural temperature development, mean annual (urban and rural) temperatures and UHI values were derived for a period of up to 30 years, namely from 1980 to 2011 (Modena, Prague, Stuttgart, Warsaw), from 1994 to 2011 (Vienna, Padua), from 2000 to 2011 (Budapest).

Table 3.3 provides an overview of the time periods used for both the short-term and the long-term analyses.

3.3 Short-Term Analyses of the Observations

Figure 3.1 shows the cumulative frequency distribution of UHI values for the participating cities for the aforementioned summer reference week. Figures 3.2 and 3.3 show for a reference summer day (representing the reference week) the hourly values of urban temperature and the hourly UHI values respectively.

Table 3.3 Overview for the data sets used for the analysis

	Reference week	Long-term climate data	
		Urban station	Rural station
Budapest	20–26.8.2011	2000–2011	2000–2011
Ljubljana	20–26.8.2011	1980–2011	1980–2011
Modena	20–26.8.2011	1980–2010	1980–2009
Padua	18–24.8.2011	1994–2011	1994–2011
Prague	8–14.7.2010	1980–2011	1980–2011
Stuttgart	20–26.8.2011	1981–2011	1980–2011
Vienna	20–26.7.2011	1994–2011	1994–2011
Warsaw	9–15.6.2008	1980–2011	1980–2011

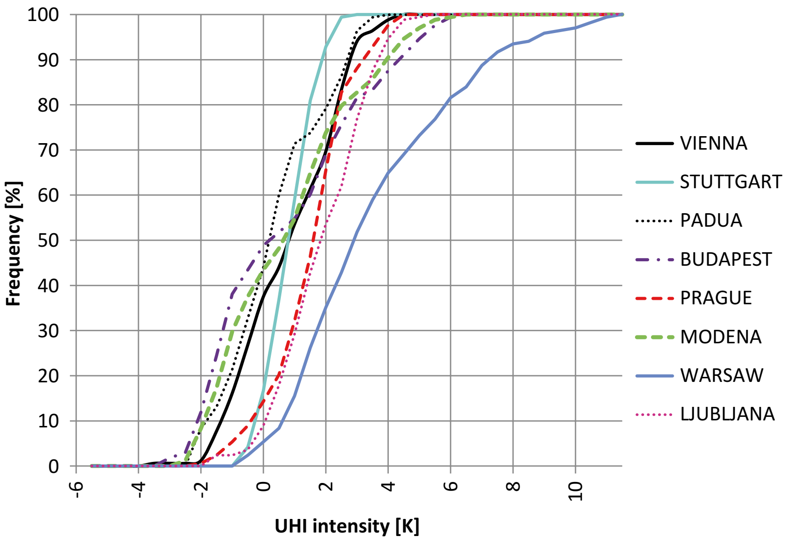

Fig. 3.1 Cumulative frequency distribution of UHI intensity for a one week summer period

The reference week data clearly demonstrate the existence and significant magnitude of the UHI effect in participating cities, especially during the night hours (Fig. 3.3). However, the time-dependent UHI patterns vary considerably across the participating cities. In Warsaw, for example, UHI intensity level ranges from around 1 K during daytime to almost 7 K during the night, while in Stuttgart levels are rather steady, ranging from 1 K to 2 K. The UHI pattern differences are also visible in the cumulative frequency distribution curves of Fig. 3.1. In this Figure, a shift to the right denotes a larger UHI magnitude.

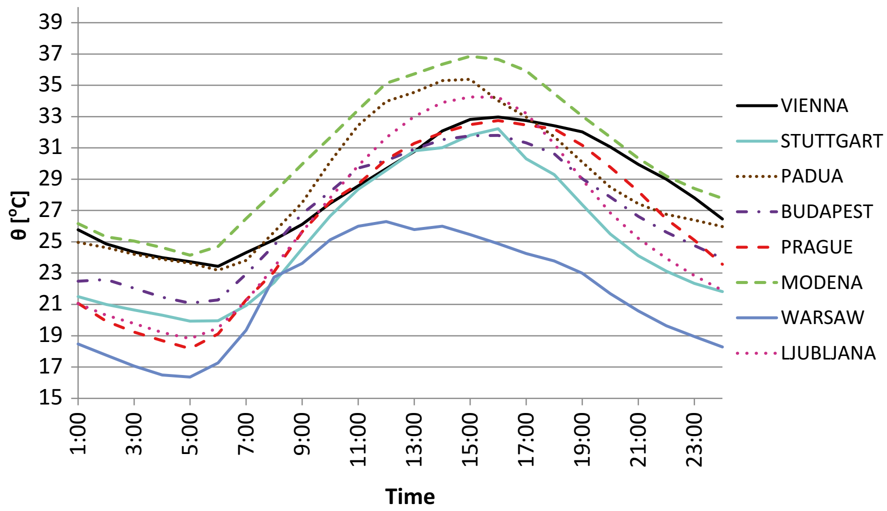

Fig. 3.2 Mean hourly urban temperature for a reference summer day

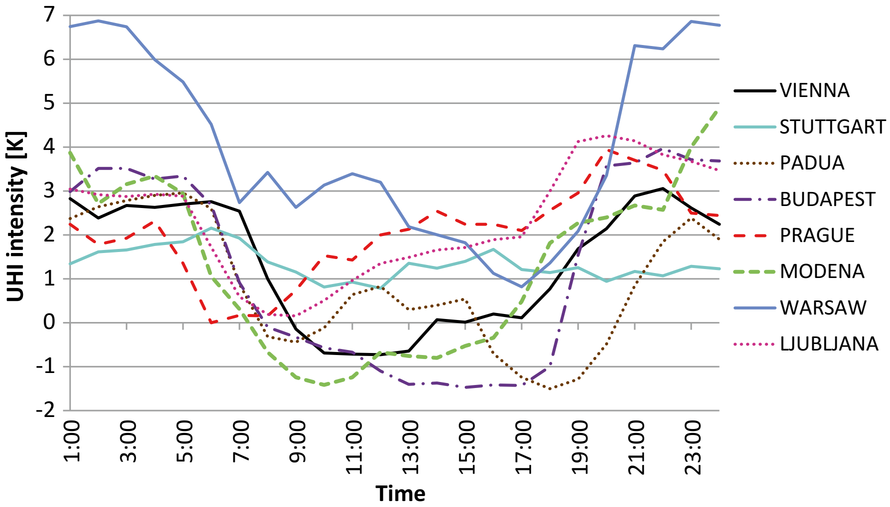

Fig. 3.3 Mean hourly UHI intensity distribution for a reference summer day

3.4 Long-Term Analyses of the Observations

Figures 3.4 and 3.5 show the (mean annual) urban and rural temperatures respectively over a period of 30 years. Figures 3.6 and 3.7 show the long-term UHI intensity trend over the same period. The historical temperature records suggest an upward trend concerning both urban and rural temperatures (see Figs. 3.4 and 3.5). Consistent with regional and global temperature trends, a steady increase in rural temperatures of up to about 2.5 K can be observed in all selected cities with the exception of Budapest. This might be due to the small sample of data set obtained, as this particular weather station was installed in the year of 2000. In the same 30-years period, the mean annual urban temperature rose somewhere between 1 K (Stuttgart) and 3 K (Warsaw). A number of factors may have contributed to this trend, namely increase in population, energy use, anthropogenic heat production, and physical changes in the urban environment (e.g., more high-rise buildings, increase in impervious surfaces). It should be noted that, while both rural and urban temperatures have been increasing, the value of the UHI intensity has been rather steady. Our data suggest increasing UHI intensity trends in Warsaw and Ljubljana, whereas a slight decrease can be discerned from Stuttgart and Prague data (Figs. 3.6 and 3.7).

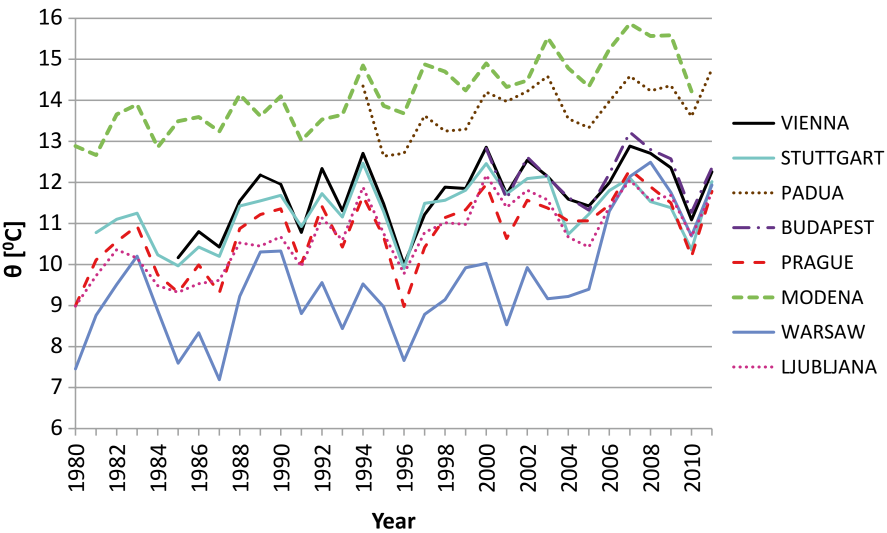

Fig. 3.4 Development of (mean annual) urban temperatures over a period of 30 years

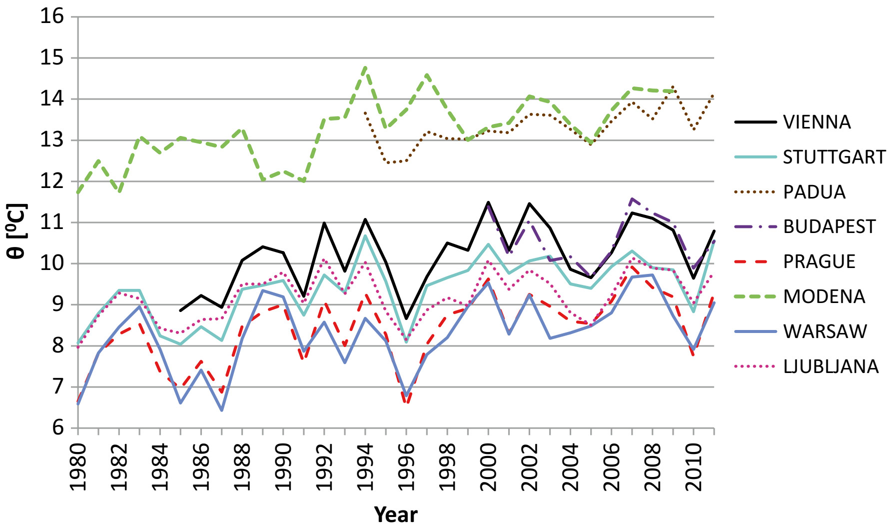

Fig. 3.5 Development of (mean annual) rural temperatures over a period of 30 years

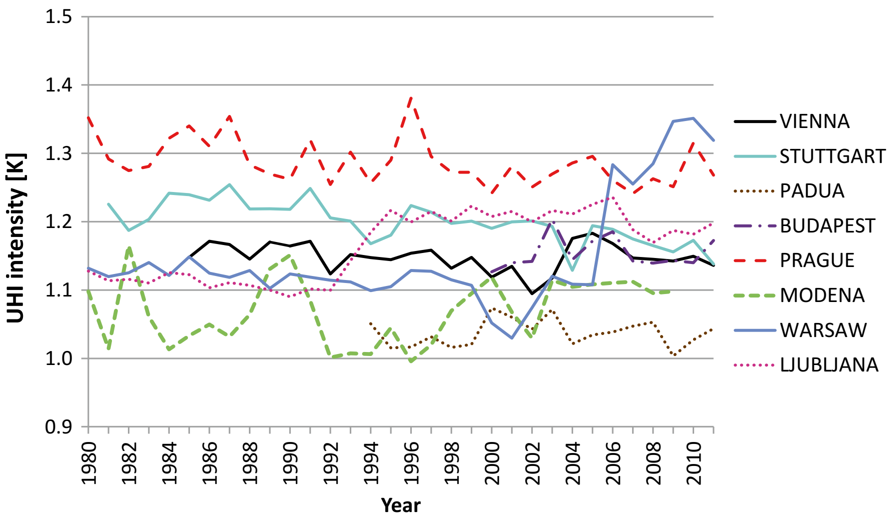

Fig. 3.6 Long-term development of the UHI intensity over a period of 30 years

3.5 Modelling Efforts

Urban microclimate is considered to be a cumulative effect of several circumstances, including small-scale processes such as combustion process of vehicles and meso-scale interactions such as atmospheric forces. To properly model and analyse

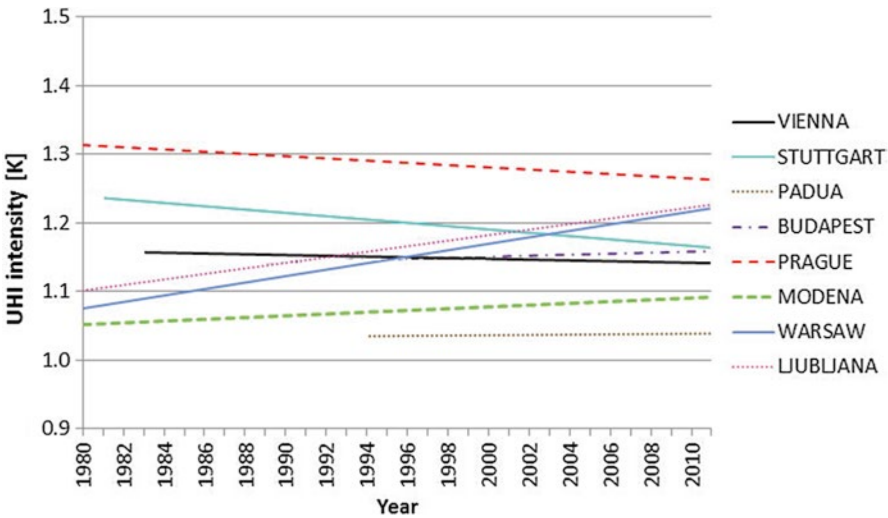

Fig. 3.7 Long-term UHI intensity trend over a period of 30 years

these effects, computational tools must consider them concurrently and in an integrated fashion. Hence detailed and complex simulation approaches are needed that have the potential to incorporate multiple aspects including hygro-thermal processes and related human comfort issues. The resulting improved predictive performance of proper computational tools would thus provide valuable feedback to planers and decision makers in confronting the UHI phenomenon.

An increasing number of tools are becoming available for microclimatic modelling of urban areas (Mirzaei and Haghighat 2010). Some tools are rather limited in terms of the range of pertinent variables they consider. Other, more detailed tools display limitations in terms of domain size and resolution. Nonetheless, numerical models still present a valuable resource for the assessment of complex thermal processes in the urban field. Within the context of this contribution, we focus on a state of art CFD-based numeric simulation environment ENVI-met (Huttner and Bruse 2009). This tool was selected as it has the capability to simulate the urban micro-climate while considering a relatively comprehensive range of factors (building shapes, vegetation, different surface properties). The high-resolution output generated by this tool includes air, soil, and surface temperature, air and soil humidity, wind speed and direction, short wave and long wave radiation fluxes, and other important microclimatic information.

Project partners undertook an extensive modelling effort including the following steps. First, a specific area within each city was selected. The idea was to select areas that are either targeted for the implementation of mitigation measures or represent likely candidates for such measures (“pilot action areas”). Second, these areas were specified in detail with regard to required model input information (i.e., geometric and semantic properties). Third, the existing microclimatic circumstances

Table 3.4 Summary of envisioned mitigation measures

	Scenario 1	Scenario 2	Scenario 3	Scenario 4	Scenario 5
Budapest	Green area + Water bodies	Trees	–	–	–
Ljubljana	Green area	Water bodies	–	–	–
Modena	Green area	Cool walls	Green roofs	Pervious ground	Cool roofs
Padua	Green area + Trees	Cool pavements	Cool roofs	S1 + Cool pavements	–
Prague	New urban develoment	Green roofs	–	–	–
Stuttgart	Green area	Trees	Water bodies	–	–
Vienna	Trees	Green roofs	Combined	–	–
Warsaw	Green area + Trees + Green roofs	S1 + Pervious pavements	–	–	–

for these areas (base case) were modelled using the aforementioned simulation environment. Fourth, candidate mitigation measures were defined for each of these areas (see Table 3.4 for an overview). Fifth, the envisioned mitigation measures were virtually implemented in the simulation environment and corresponding output was generated. Sixth, the base case conditions were compared with the predicted post-mitigation circumstances to provide a quantitative basis for the evaluation of the effectiveness of the envisioned mitigation measures.

To illustrate the kinds of information and analyses that can be obtained from the modelling process, relevant results are provided below for three cities, namely Vienna, Padua, and Warsaw. Toward this end, Figs. 3.8, 3.9, and 3.10 show the mean hourly temperature in the course of a reference summer day in Vienna, Padua, and Warsaw for the base case and three mitigation scenarios. Figures 3.11, 3.12, and 3.13 show the corresponding temperature differences between the base case and the applicable mitigation scenarios in the course of a reference summer day. These results point to the potential of various mitigation measures to reduce air temperature levels in hot summer days in the selected cities. As it could be expected, different mitigation measures display different levels of impact. For example, in case of the targeted area in Vienna, green roofs do not appear to noticeably influence the air temperature in the urban canyon. Trees, on the other hand, do impact the air temperature. The combination of these two measures proved in this case to be most effective. With regard to the temporal pattern of the effects, it can be noted that the difference in air temperature is more pronounced during evening and night hours.

To further investigate the temporal nature of UHI intensity values (and their sensitivity to various mitigation measures), we introduced the concepts of Cumulative Temperature Increase (CTI) and Cumulative Temperature Decrease (CTD). CTI and CTD are computed as the cumulative sum of all positive and negative values respectively in the course of a reference day:

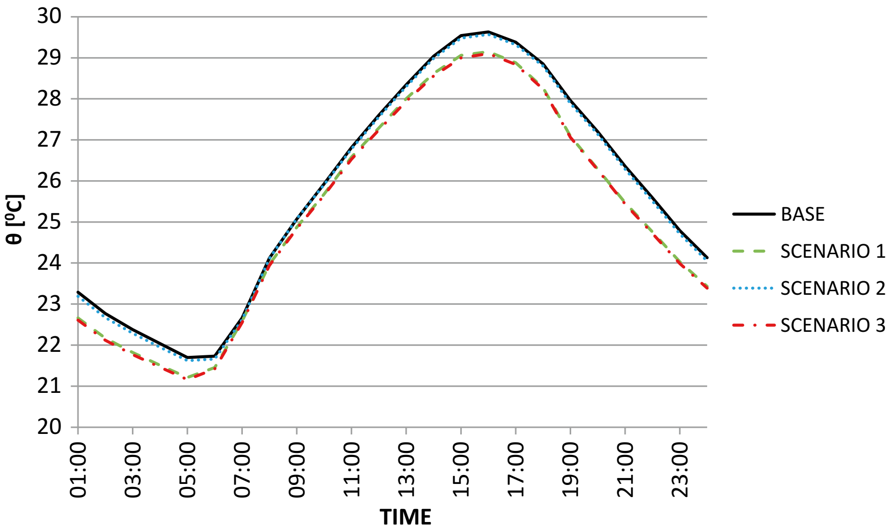

Fig. 3.8 Mean hourly temperature in the course of a reference summer day in Vienna for the base case and three mitigation scenarios

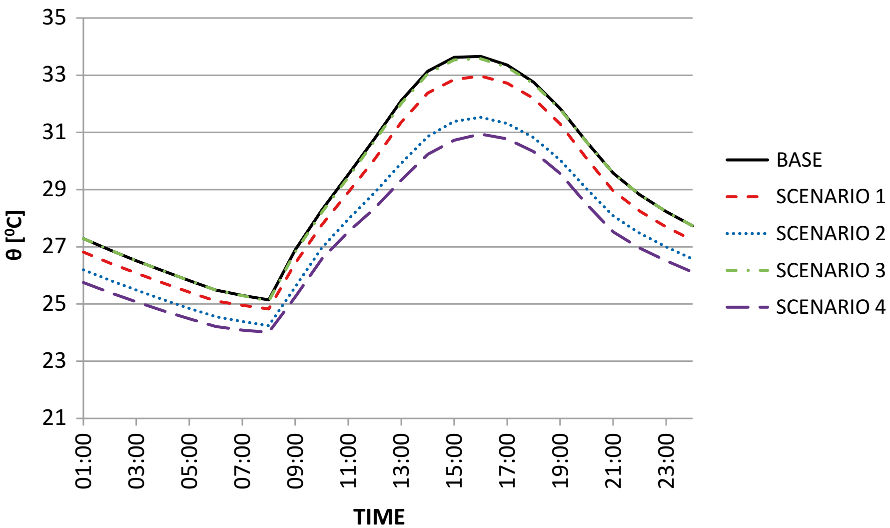

Fig. 3.9 Mean hourly temperature in the course of a reference summer day in Padua for the base case and four mitigation scenarios

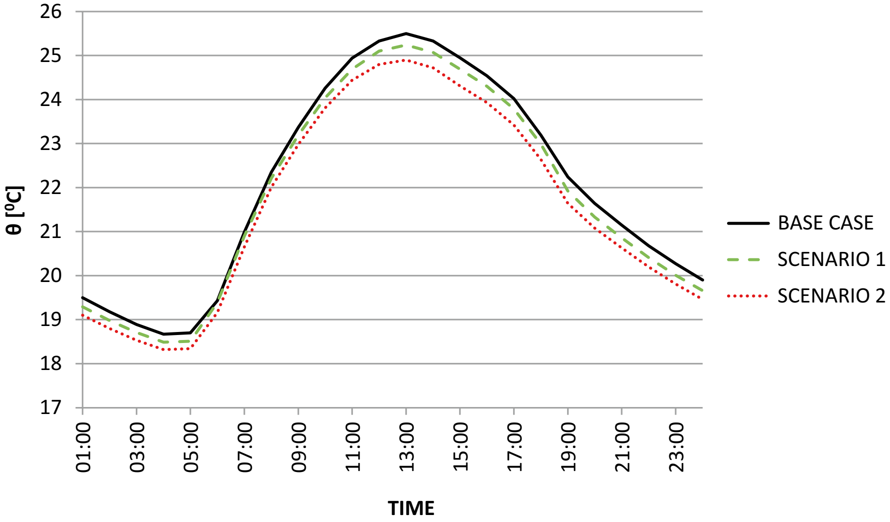

Fig. 3.10 Mean hourly temperature in the course of a reference summer day in Warsaw for the base case and two mitigation scenarios

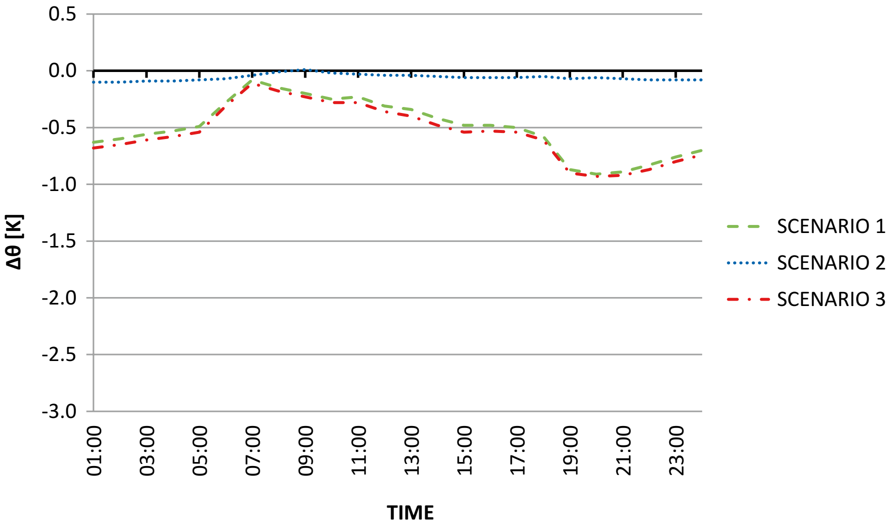

Fig. 3.11 Temperature difference between the base case and three mitigation scenarios in the course of a reference summer day in Vienna

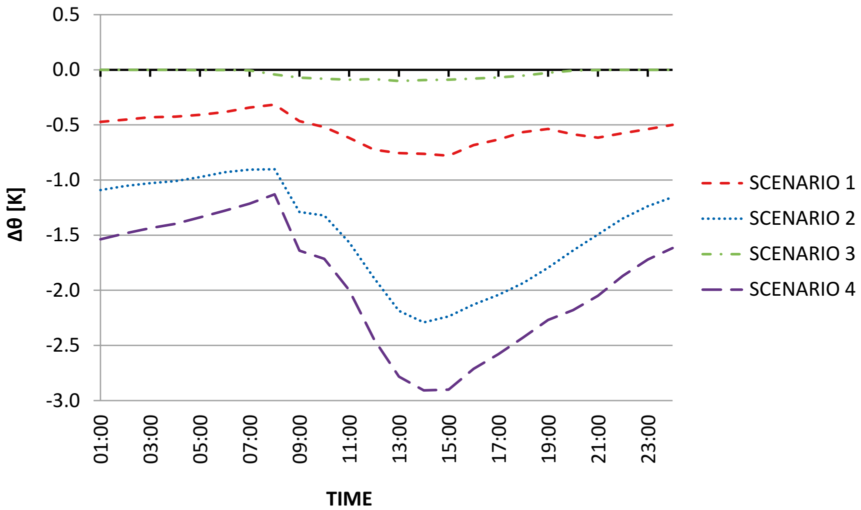

Fig. 3.12 Temperature difference between the base case and four mitigation scenarios in the course of a reference summer day in Padua

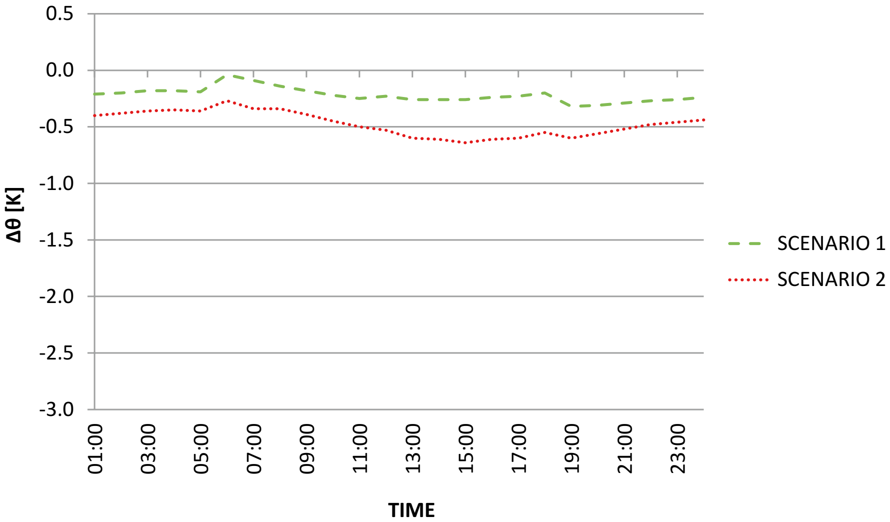

Fig. 3.13 Temperature difference between the base case and two mitigation scenarios in the course of a reference summer day in Warsaw

Table 3.5 Summary of predicted CTD and CTI values for summer and winter seasons for all mitigation measures in all cities

City	Mitigation measures		Summer		Winter	
			CTD	CTI	CTD	CTI
Budapest	S1	New urban development + Green area + Water bodies	16	7	18	0
	S2	Trees	2	0	1	0
Ljubljana	S1	Green area	1	0	2	0
	S2	Water bodies	1	0	0	0
Modena	S1	Green area	21	0	N/A	N/A
	S2	Cool walls	0	4	0	1
	S3	Green roofs	6	0	1	0
	S4	Pervious ground	5	0	N/A	N/A
	S5	Cool roofs	2	0	1	0
Padua	S1	Green area + Trees	13	0	1	0
	S2	Cool pavements	35	0	6	0
	S3	Cool roofs	1	0	0	2
	S5	S1 + Cool pavements	47	0	6	0
Prague	S1	New urban development	0	21	0	31
	S2	Green roofs	0	26	0	30
Stuttgart	S1	Green area	7	0	99	0
	S2	Trees	7	1	0	6
	S3	Water bodies	0	0	11	0
Vienna	S1	Trees	12	0	1	0
	S2	Green roofs	1	0	0	0
	S3	Combined	13	0	1	0
Warsaw	S1	Green area + Trees + Green roofs	5	0	0	0
	S2	S1 + Pervious pavements	11	0	1	0

$$CTI = \sum_{i=1}^{24} \left(\theta_{B,i} - \theta_{S,i}\right) \text{forallintervalswhen} \theta_{B,i} < \theta_{S,i} \quad (3.1)$$

$$CTD = \sum_{i=1}^{24} \left(\theta_{B,i} - \theta_{S,i}\right) \text{ forallintervalswhen} \theta_{B,i} > \theta_{S,i} \quad (3.2)$$

A summary of the results (predicted CTD and CTI values for summer and winter seasons for all mitigation measures in all cities) is provided in Table 3.5.

These results illustrate the potentially significant utility of the modelling tools and approaches for decision making processes pertaining to the proper choice of UHI mitigation measures. However, as with other areas of applied numerical modelling, certain important challenges must be addressed. One issue is related to the rather extensive time and computational resources that are necessary for proper

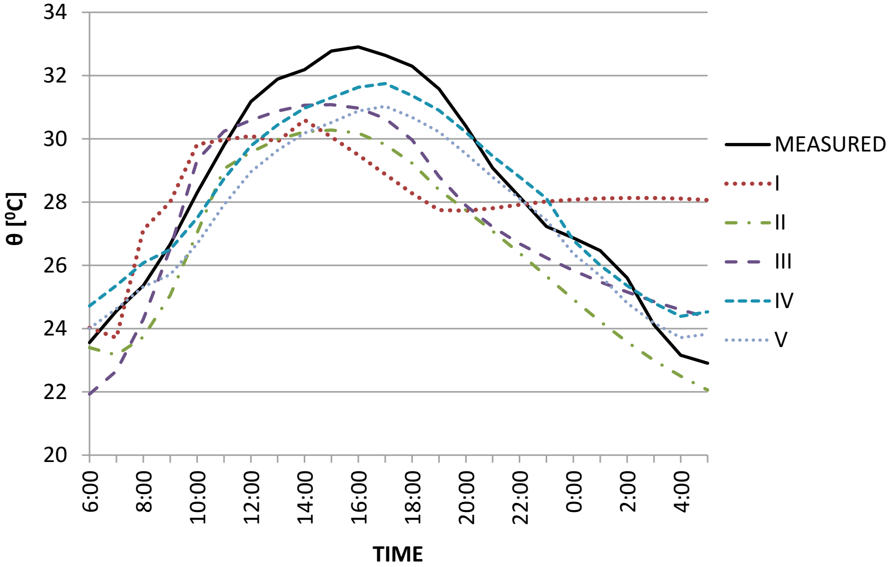

Fig. 3.14 Comparison of the measured mean hourly temperature in the course of a summer day (22nd July 2010) in Vienna with simulation results conducted with various simulation setting and forcing parameter options (cases I to V)

deployment of complex simulation tools. A second challenge pertains to the issue of model reliability: Even highly detailed and mathematically consistent simulation tools may yield erroneous results given incomplete (or inaccurate) input data.

The high level of domain complexity involved in urban microclimate modelling aggravates this model reliability problem. To exemplify this circumstance, consider the simple case of predicting the air temperature in a specific location in the city of Vienna. In this case, the actual air temperature measurements at this location were compared with simulated results, whereby different tool versions and settings as well as different forcing parameters were considered. The results (see Fig. 3.14) suggest that predictions based on computation may significantly deviate from actual measurements, thus undermining the practical usability of modelling tools. An important approach to address the model reliability issues focuses on model calibration potential (Maleki et al. 2014).

In addition to numerical modelling, we explored the potential of simple empirically-based relationships between fundamental features of the urban setting (morphology, materials) and basic microclimatic variables. Such relationships would not only provide efficient means for rough estimations of the effectiveness of mitigation measures, but would also provide a basic plausibility check for the results of numerical computation. Hence, within the framework of the project, we developed a systematic framework toward definition and derivation of fundamental variables of a selected urban area. These variables are hypothesized to influence UHI and the urban microclimate variance. They pertain to both geometric (morphological) and semantic (material-related) urban features and are captured within a formal and systematic framework.

3.6 A Systematic Framework for the Representation of Urban Variables

Within the UHI project, a systematic framework was developed (Mahdavi et al. 2013) to assess – for a specific urban location, hereafter referred to as urban unit of observation (U2O) – the urban heat island phenomenon, to specify potential mitigation measures, and to evaluate such measures via adequate empirically-based calculation methods. The framework involves the following steps:

(i) Definition of "Urban Units of Observation" (U2O): These are properly bounded areas within an urban setting selected as the target and beneficiary of candidate UHI mitigation measures;
(ii) Description of the status quo of U2O in terms of a structured set of geometric and physical properties;
(iii) Specification of the existing extent of UHI in terms of proper indicators;
(iv) Specification of the candidate mitigation measures in terms of projected changes to the geometric and/or physical properties captured in step ii above;
(v) Prediction of the effect of mitigation measures using empirically-based calculation methods;
(vi) Expression of the mitigation measures' impact in terms of predicted changes in the extent of UHI.

Table 3.6 Variables to capture the geometric properties of an U2O

Geometric properties	Definition
Sky view factor	Fraction of sky hemisphere visible from ground level
Aspect ratio	Mean height-to-width ratio of street canyons
Built area fraction	The ratio of building plan area to total ground area
Unbuilt area fraction	The ratio of unbuilt plan area to total ground area
Impervious surface fraction	The ratio of unbuilt impervious plan area to total ground area
Pervious surface fraction	The ratio of unbuilt impervious surface area to total ground area
Equivalent building height	The ratio of built volume (above terrain) to total ground area
Built surface fraction	The ratio of total built surface area to total built area
Wall surface fraction	The total area of vertical surfaces (walls)
Roof surface fraction	The total area of horizontal surfaces (roofs)
Effective mean compactness	The ratio of built volume (above terrain) to total surface area (built and unbuilt)
Mean sea level	Average height above sea level

Table 3.7 Variables to capture the surface and material properties of an U2O

Surface/material properties	Definition
Reflectance/albedo	Fraction of reflected direct and diffuse shortwave radiation
Emissivity	Ability of a surface to emit energy by radiation (longwave)
Thermal conductivity	Property of a material's ability to conduct heat, given separately for impervious and pervious materials
Specific heat capacity	Amount of heat required to change a body's temperature by a given amount, given separately for impervious and pervious materials
Density	Mass contained per unit volume, given separately for impervious and pervious materials
Anthropogenic heat output	Heat flux density from fuel combustion and human activity (traffic, industry, heating and cooling of buildings, etc.)

In this framework, the notion of U2O is applied to systematically address the local variation of the urban climate throughout a city. A spatial dimension (diameter) of approximately 400–1000 m has been targeted for U2O.

As the urban microclimate is believed to be influenced by different urban morphologies, structures, and material properties, a set of related variables were identified and included in our framework (Tables 3.6 and 3.7) based on past research (Nowak 2002; Piringer et al. 2002; Burian et al. 2005; Ali-Toudert and Mayer 2006) and our own investigations (Mahdavi et al. 2013; Kiesel et al. 2013).

The geometric properties are meant to capture the urban morphology of an U2O. The physical properties describe mainly the thermal characteristics of urban surfaces. These properties are often considered as fundamental factors in view of the heat balance of urban systems (Rosenfeld et al. 1995).

To derive the specific values of the U2O variables for the selected urban areas, we used data provided by the city of Vienna in a form of a Digital Elevation Model (DEM). The DEM consisted of a terrain and a surface model, including building footprints in form of closed polygons associated with building height data (which indicates the height of the building eaves). QGIS (Quantum GIS 2013), an open source Geographic Information System, was used to visualize, manage, and analyse the data. A specific set of algorithms was developed (Glawischnig et al. 2014) and further used for the quantitative analysis of the microclimatic attributes.

To exemplify and illustrate the application of the aforementioned algorithms and procedures, Fig. 3.15 depicts computed values of a selected set of geometric and semantic variables for four locations across Vienna. The selected locations include both low-density suburban and high-density urban typologies in Vienna (Table 3.8). Given the specific arrangement of the respective scales in this representation (descending versus ascending order of the scale numbers), it can support the recognition of distinct differences between the selected locations.

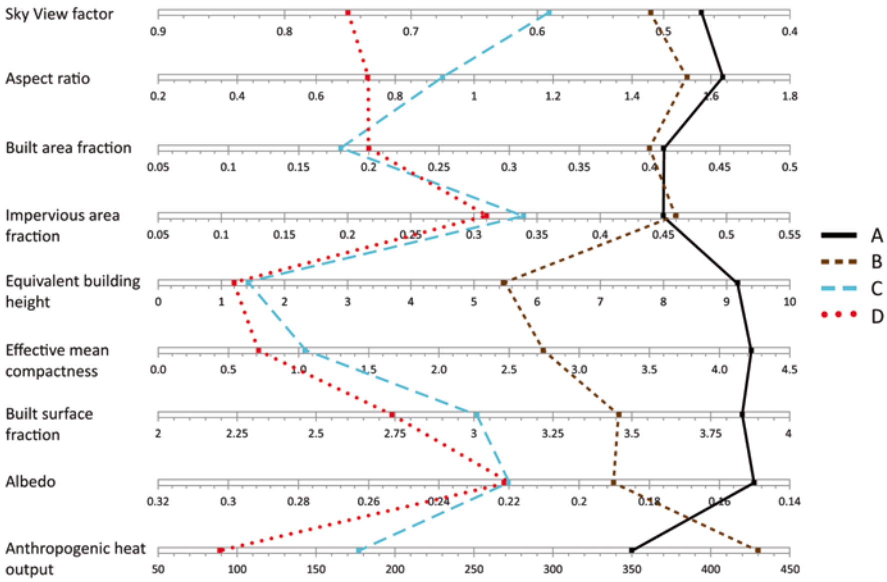

Fig. 3.15 The computed values of a number of U2O variables for the urban areas around the aforementioned five weather station locations

Table 3.8 Information regarding the selected locations in the city of Vienna

	Name	Type	Elevation
A	Innere Stadt	Urban (city center)	177 m
B	Gaudenzdorf	Urban	179 m
C	Hohe Warte	Urban (peripheral)	198 m
D	Donaufeld	Suburban	161 m

A clear shift to the left in Fig. 3.15 denotes a more suburban character, while the shift to the right denotes a more urban character.

Once U2Os and their respective variables are derived, the existence and extent of the correlations between urban microclimate variance and the U2O variables are explored. These statistically significant correlations could provide a useful basis toward developing empirically-based predictive models. Such models could support, amongst other things, decision making processes with regard to the selection of appropriate mitigation measures that are intended to address the UHI phenomena.

Ongoing work in this area involves the collection of information on urban microclimate variance and the analysis of its hypothesised relationship to U2O variables. While certain U2O variables (impervious surface fraction, anthropogenic heat emission) are hypothesised to positively correlate with indicators of UHI phenom-

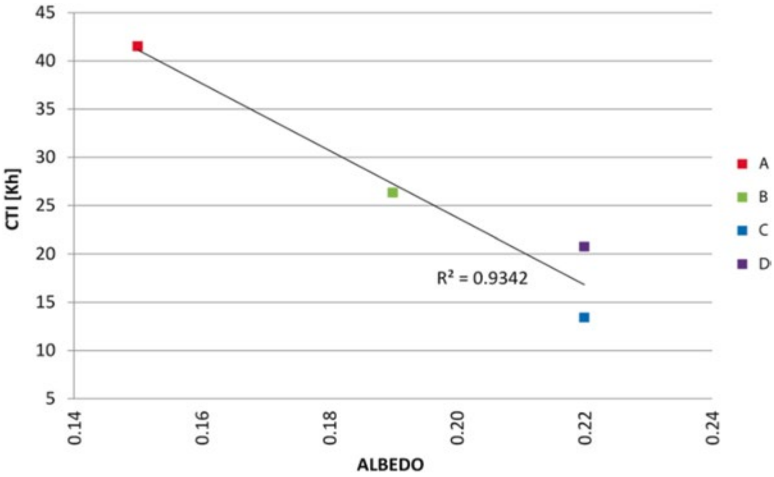

Fig. 3.16 Correlation between the albedo and CTI values for summer period for selected areas (A to D) in Vienna

enon, others (sky view factor, albedo) are more likely to display a negative correlation. While the state of progress in this area has not reached the point to warrant solid and generally valid relationships, initial findings appear to be promising. For example, Fig. 3.16 illustrates the relationship between urban surface albedo (determined for four location across Vienna) and the measured summer-time CTI in those areas.

3.7 Conclusion

We presented the results of EU-supported project concerned with the extent of the UHI phenomena in a number of Central European cities. The objectives of this project are to provide a common understanding of the UHI effects and to conceive and evaluate appropriate mitigation and adaptation measures. Short-term and long-term data with regard to urban and rural temperatures demonstrate the existence and significant magnitude of the UHI effect in a number of Central European cities. Furthermore observations based on hourly data display distinguished patterns implying larger UHI intensities during the night hours. To address the need for effective means of evaluating and mitigating UHI effects a comprehensive modelling effort was undertaken. Thereby, the ramifications of potential mitigation measures in selected areas of the participating cities were investigated using advance numeric modelling tools and techniques. Moreover, a systematic framework was developed and tested, which proposed and tested a number of geometric (morphological) and semantic (material-related) variables of the urban environment. These variables are hypothesized to influence UHI and the urban microclimate variance. Currently, the suggest link is being explored and statistically analysed. This work is expected to not only provide empirical data for the validation of numeric models, but also to support the formulation of simplified approaches toward estimation of mitigation measures effectiveness in view of UHI phenomena.

Acknowledgements This project was funded in part within the framework of the EU-Project "Development and application of mitigation and adaptation strategies and measures for counteracting the global Urban Heat Island phenomenon" (Central Europe Program, No 3CE292P3).

References

Akbari, H. (2005). *Energy saving potentials and air quality benefits of urban heat island mitigation*. Berkeley: Lawrence Berkeley National Laboratory.

Akbari, H., Pomerantz, M., & Taha, H. (2001). Cool surfaces and shade trees to reduce energy use and improve air quality in urban areas. *Solar Energy, 70*(3), 295–310.

Alexandri, E. (2007). *Green cities of tomorrow?* Paper presented at the Sustainable Construction, Materials and Practices, SB07, Portugal.

Ali-Toudert, F., & Mayer, H. (2006). Numerical study on the effects of aspect ratio and orientation of an urban street canyon on outdoor thermal comfort in hot and dry climate. *Buildings and Environment, 41*, 94–108.

Arnfeld, A. J. (2003). Two decades of urban cli-mate research: A review of turbulence, exchanges of energy and water, and the urban heat island. *International Journal of Climatology, 23*(1), 1–26.

Blazejczyk, K., Bakowska, M., Wieclaw, M. (2006). *Urban heat island in large and small cities*. Paper presented at the 6th international conference on urban climate, Göteborg, Sweden.

Burian, S., Suk Han, W., & Brown, M. J. (2005). *Morphological analysis using 3D building databases: Oklahoma City*. Oklahoma: Los Alamos National Laboratory.

Gaffin, S. R., Rosenzweig, C., Khanbilvardi, R., Parshall, L., Mahani, S., Glickman, H., Goldberg, R., Blake, R., Slosberg, R. B., & Hillel, D. (2008). Variations in New York City's urban heat island strength over time and space. *Theoretical and Applied Climatology, 94*, 1–11.

Glawischnig, S., Kiesel, K., Mahdavi, A. (2014, May). *Feasibility analysis of open-government data for the automated calculation of the micro-climatic attributes of urban units of observation in the city of Vienna*. Paper presented at the 2nd ICAUD International Conference in Architecture and Urban Design, Epoka University, Tirana, Albania.

Grimmond, C. S. B. (2007). Urbanization and global environmental change: Local effects of urban warming. *Cities and Global Environmental Change, 173*(1), 83–88.

Grimmond, C. S. B., & Oke, T. R. (1999). Heat storage in urban areas: Local-scale observations and evaluation of a simple model. *Journal of Applied Meteorology, 38*(7), 922–940.

Grimmond, C. S. B., Cleugh, H., & Oke, T. R. (1991). An objective urban heat storage model and its comparison with other schemes. *Atmospheric Environment, 25B*(3), 311–326.

Harlan, S. L., & Ruddell, D. M. (2011). Climate change and health in cities: Impacts of heat and air pollution and potential co-benefits from mitigation and adaptation. *Current Opinion in Environmental Sustainability, 3*(3), 126–134.

Hart, M. & Sailor, D.J. (2007, September). *Assessing causes in spatial variability in urban heat island magnitude*. Paper presented at the Seventh Symposium on the Urban Environment, San Diego, CA

Huttner, S. & Bruse, M. (2009, June–July). *Numerical modelling of the urban climate – A preview on ENVI-met 4.0*. Paper presented at the 7th International Conference on Urban Climate ICUC-7, Yokohama, Japan.

Kiesel, K., Vuckovic, M., Mahdavi, A. (2013). *Representation of weather conditions in building performance simulation: A case study of microclimatic variance in Central Europe*. Paper presented at the 13th International Conference of the International Building Performance Simulation Association, IBPSA, France.

Kleerekoper, L., van Esch, M., & Salcedo, T. B. (2012). How to make a city climate-proof, addressing the urban heat island effect. *Resources, Conservation and Recycling, 64*, 30–38.

Mahdavi, A., Kiesel, K., Vuckovic, M. (2013, April). *A framework for the evaluation of urban heat island mitigation measures*. Paper presented at the SB13 Munich Conference, Germany.

Maleki, A., Kiesel, K., Vuckovic, M., & Mahdavi, A. (2014). Empirical and computational issues of microclimate simulation. Information and Communication Technology. *Lecture Notes in Computer Science, 8407*, 78–85.

Mirzaei, P. A., & Haghighat, F. (2010). Approaches to study urban heat island – Abilities and limitations. *Building and Environment, 45*(10), 2192–2201.

Nowak, D. J. (2002). *The effects of urban trees on air quality*. Syracuse: USDA Forest Service.

Oke, T. R. (1972). City size and the urban heat island. *Atmospheric Environment, 7*(8), 769–779.

Oke, T. R. (1981). Canyon geometry and the nocturnal urban heat island comparison of scale model and field observations. *Journal of Climatology, 1*, 237–254.

Piringer, M., Grimmond, C. S. B., Joffre, S. M., Mestayer, P., Middleton, D. R., Rotach, M. W., Baklanov, A., De Ridder, K., Ferreira, J., Guilloteau, E., Karppinen, A., Martilli, A., Masson, V., & Tombrou, M. (2002). Investigating the surface energy balance in urban areas – Recent advances and future needs. water. *Air and Soil Pollution: Focus, 2*(5–6), 1–16.

Quantum GIS. (2013). http://www.qgis.org/en/site/

Rosenfeld, A. H., Akbari, H., Bretz, S., Fishman, B. L., Kurn, D. M., Sailor, D. J., & Taha, H. (1995). Mitigation of urban heat islands: Materials, utility programs, updates. *Energy and Buildings, 22*(3), 255–265.

Shishegar, N. (2013). Street design and urban microclimate: Analysing the effects of street geometry and orientation on airflow and solar access in urban canyons. *Journal of Clean Energy Technologies, 1*(1), 52–56.

Taha, H. (1997). Urban climates and heat islands: Albedo, evapotranspiration, and anthropogenic heat. *Energy and Buildings, 25*(2), 99–103.

Unger, J. (2004). Intra-urban relationship between surface geometry and urban heat island: Review and new approach. *Climate Research, 27*, 253–264.

Voogt, J. A. (2002). Urban heat island. *Encyclopedia of Global Environmental Change, 3*, 660–666.